IEICE Proceeding Series

Bifurcation Dynamics of an Intrinsic Localized Mode in a Driven 1-D Nonlinear Lattice

M. Sato, Y. Takao, Y. Sada, W. Shi, S. Shige, A. J. Sievers

Vol. 1 pp. 407-410
Publication Date: 2014/03/17
Online ISSN: 2188-5079

Bifurcation Dynamics of an Intrinsic Localized Mode in a Driven 1-D Nonlinear Lattice

M. Sato†, Y. Takao†, Y. Sada†, W. Shi†, S. Shige†, and A. J. Sievers‡

†School of Natural Science and Technology, Kanazawa University
Kakumamachi, Kanazawa, Ishikawa, 920-1192 Japan
‡ Laboratory of Atomic and Solid State Physics, Cornell University
Ithaca, NY 14853-2501, USA
Email: msato@kenroku.kanazawa-u.ac.jp

Abstract– The experimental linear response spectrum of an auto-resonant (AR) intrinsic localized mode (ILM) in a driven 1-D cantilever array is composed of several resonances including a phase mode of the AR-ILM. This AR state is stable in a finite frequency range between the upper and lower bifurcation frequencies. Here we examine the robustness of the lower frequency point to lattice perturbations. In the intrinsic state the even linear localized mode (LLM) crosses the phase mode and the transition occurs when the phase mode intersects the odd symmetry band mode. When an impurity mode is introduced into the lattice near the even LLM it interacts with the phase mode, and the lower bifurcation frequency of the ILM is now shifted to the point where these two linear modes coalesce.

1. Introduction

As a driven mechanical oscillator becomes smaller in size, nonlinearity plays a more important role. In a micromechanical cantilever array nonlinearity plus discreteness can give rise to vibrational localization. Such an intrinsic localized mode (ILM), also called a discrete breather, has been predicted theoretically and observed experimentally.[1-4] These nonlinear localized modes have attracted attention both because of fundamental interest and also because of possible practical applications. [5-18]

Experimentally, a stationary ILM can be maintained in steady state using a driver to compensate for damping.[5-7] In this state the ILM is frequency locked, and a so called auto-resonance (AR) state is achieved where the driver frequency controls the ILM amplitude.[19-22] Such a stable state is only possible over a well defined frequency region[10, 16] and the two frequency boundaries are identified as bifurcation points.

By measuring the linear response spectrum of an ILM as a bifurcation point is approached we have been able to characterize the underlying dynamics of the transition. [16] Two linear modes are observed, a phase mode and an even linear localized mode (LLM).[8] The phase mode amplitude diverges at both the upper and lower bifurcation points when its frequency intersects the driver frequency or its frequency intersects the highest frequency band mode.

The even-LLM crosses the phase mode near the lower bifurcation point without any interaction. In this paper, we introduce an additional impurity mode on the lattice to probe the robustness of the lower bifurcation point.

2. Experiments

Figure 1 shows the experimental set up for the pump-probe measurement. The pump driver generates the ILM and keeps it in the AR state. The probe driver is used to apply a sinusoidal perturbation to the system. The displacement near the ILM is detected by a combination of the laser diode and a position sensitive detector, and recorded with a digitizer. The recorded signal is Fourier transformed to produce a spectrum. To have high resolution near the pump frequency, the signal is down converted using a mixer and a local oscillator. By changing the probe driver frequency step wise, and measuring perturbed spectra at these frequencies, a probe response spectrum is then deduced. This method is more tedious than the one we reported earlier [16], where we have used a lock-in amplifier instead of the digitizer. However, this method reveals the overall spectral response.

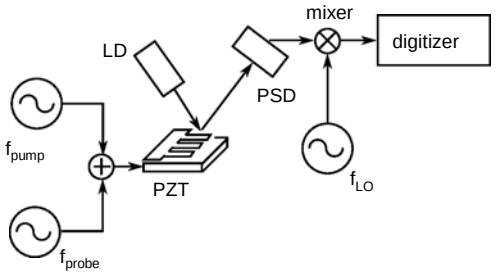

Fig. 1 Experimental set up for the pump-probe measurement with a uniform probe perturbation. The cantilever array is located in a vacuum chamber (not shown). Pump and probe drivers excite the PZT, which shakes the array to produce the acceleration force on it. The pump driver maintains the ILM. A diode laser is focused on one cantilever near the ILM. The position sensitive detector (PSD) converted the displacement signal to voltage. After the signal frequency is down converted to produce fine spectral resolution, the cantilever displacement is recorded. The weak probe driver is used to apply a sinusoidal perturbation to the array.

Figure 2(a) shows the two dimensional map made from such spectra. There are two lines crossing at the center whose position is on the line $f_{FFT} = f_{probe}$ and $f_{FFT} = 2f_{pump} - f_{probe}$. Intensities of these lines are plotted on Fig. 2(b). They consist of the response spectrum and a four-wave mixed spectrum. We can confirm that the curves in Fig. 2(b) are the response to the probe perturbation, because no other signal in Fig. 2(a) except structures on lines $f_{FFT} = f_{probe}$ and $f_{FFT} = 2f_{pump} - f_{probe}$.

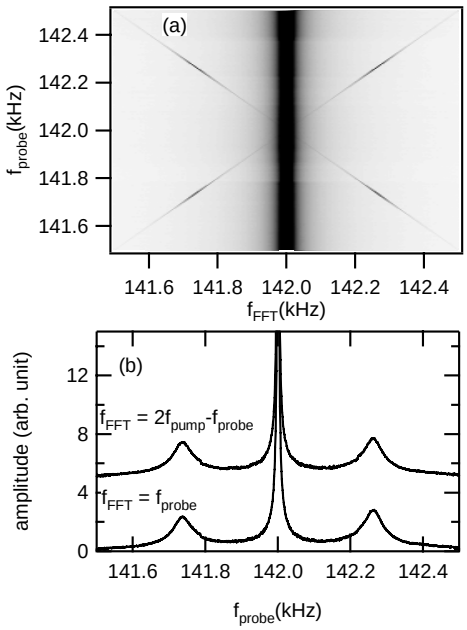

Fig. 2 (a) FFT spectra of the ILM sidebands under fixed pump excitation at 142 kHz and various probe excitation frequency. Spectra are mapped from low to high according to the probe frequency. Vertical bar is the ILM signal. Crossing lines represent signal caused by the probe driver. Pump level is 15Vpp, and probe level is 20mVpp. The dark region at 142 kHz is due to the AR-ILM vibrating at the pump frequency. (b) Probe response spectrum obtained from the line $f_{FFT} = f_{probe}$ and four-wave mixing spectrum from the line $f_{FFT} = 2f_{pump} - f_{probe}$. Two sideband peaks symmetrically located to the pump frequency is due to the phase motion of the AR-ILM.

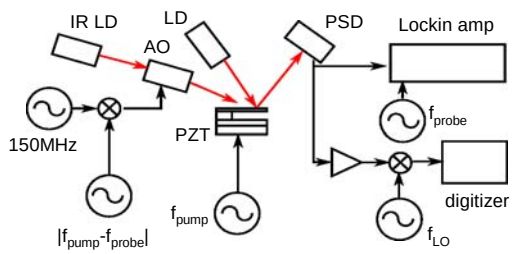

Fig. 3 Experimental set up for the pump-probe measurement with an asymmetric perturbation. An IR laser beam is modulated by an acousto-optic (AO) modulator at frequency $|f_{pump} - f_{probe}|$, and irradiates one side of the ILM. The displacement signal is analyzed either by a lock-in amplifier with a reference frequency at f_{probe} or by the digitizer.

The pair of sideband is due to the phase mode of the ILM. It is the free vibration solution which is monitored by the probe. As we reported previously, this method can only measure odd shaped modes. This is because the uniform perturbation produced by the probe cannot excite the even mode.

To see the even-mode clearly, we have added to the experiment a sinusoidal modulated laser beam that can heat a local spot on the array, producing a modulated impurity mode, which breaks the local symmetry of the ILM. Now both even symmetry and odd symmetry modes can be observed. Figure 3 shows the experimental set up. Because of a frequency bandwidth of the AO modulator, we modulated the beam power at the difference frequency $f_{mod} = |f_{pump} - f_{probe}|$, which is well below the probe frequency itself. The time dependence of the impurity mode induces both a lateral and breathing motion of the ILM. By these processes, all linear modes are observable by this method.

Figure 4 shows the map made from the digitizer signal by step changing the modulation frequency $f_{mod} = |f_{pump} - f_{probe}|$. Starting from the bottom of the figure the two dark narrow lines diverging from a point represent the signal caused by the modulated laser beam. In this case, clear signal is only observed on these two lines $f_{FFT} = f_{pump} \pm f_{mod}$ indicating that signals on these are due to the probe perturbation, excepts some fixed frequency noise that were recorded as vertical lines. The noise might be a spurious signal from the pump driver, or other fixed frequency source.

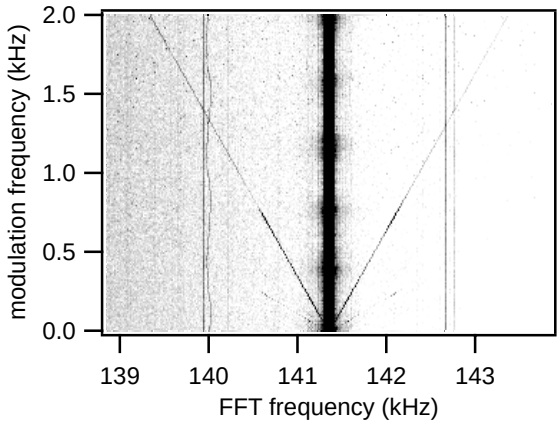

Fig. 4 FFT spectra versus the modulation frequency of the IR laser beam. Two lines at $f_{FFT} = f_{pump} \pm f_{mod}$ are response signals from the laser modulation. Thick vertical line is the ILM and other weak vertical lines are due to noise. The pump frequency was fixed at 141.35 kHz and the modulation frequency was step increased, then the cantilever motion of the ILM was recorded. The soft focused IR laser beam directed at one side of the ILM caused its asymmetric deformation and breathing vibration.

Figure 5 shows the pump frequency dependence of the probe spectra measured by the laser local heating

perturbation. The pump frequency was changed from the middle of the AR region down to the low frequency bifurcation point. The spectra are aligned from top to bottom by the pump frequency. The strong sideband pair near the center is due to the phase mode and its partner, as also shown in Fig. 2. Weaker resonance peaks outside of the phase mode approach the phase mode as the pump frequency is decreased. The strongest of these is the even LLM. The weaker one is the highest frequency band mode.

At the bottom of this figure, just before the ILM becomes unstable and disappears, the phase mode and the even mode mix and the resultant amplitude increases considerably in height.

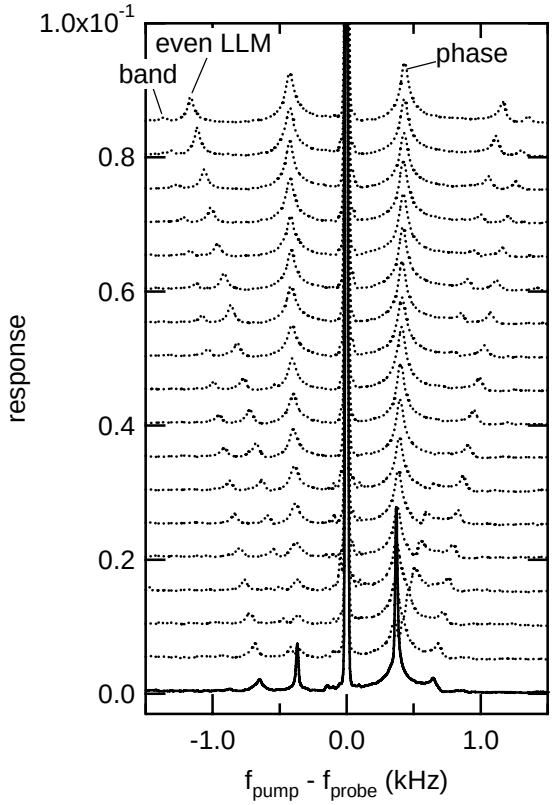

Fig. 5 Local probe response versus frequency difference for various pump frequencies, from 140.85 to 141.70 kHz with 50 Hz step from bottom to top. The soft focused, modulated IR laser beam is directed to one side of the ILM. The broken symmetry of the ILM makes the odd phase mode and the even LLM interact, as shown in the bottom trace (solid). The modulation frequency f_{mod} is scanned and the PSD signal is detected by the lock-in amplifier with the reference frequency at $f_{probe} = f_{pump} \pm f_{\mathrm{mod}}$. The sidebands ~ $\pm 425 Hz$ are the same as in Fig. 2. The broken symmetry even LLM is identified. When those two modes are coincides at the bottom (solid curve), the peak heights rapidly increase, and the ILM becomes unstable. Pump level is 14.2Vpp, and probe IR laser power is 10mW in average.

4. Discussions

In an earlier work we have shown that for the pure lattice case the lower bifurcation point occurs when the partner of the odd phase mode intersects the top most odd band mode of the lattice.[16] The current measurements show that for a perturbed lattice the result is somewhat different. By breaking the vibrational symmetry of the ILM with the introduction of an impurity mode the bifurcation frequency is shifted so that it now occurs at a higher frequency point where the even LLM and the odd phase mode coalesce. How is this possible?

To address this question first consider the translational motion of an ILM though the unperturbed lattice. It requires the ILM to change it shape from odd symmetry to even symmetry and back again as it passes through a unit cell. It is the difference in frequency between these two eigenvectors that finally traps the ILM in its most stable symmetry state as the localization strengthens. But at the lower bifurcation point the ILM envelope is fairly broad and hence only weakly trapped. In a pure lattice, an odd shaped phase mode and an even shaped LLM do not interact. However, the laser spot makes a modulated impurity mode. When this spot is placed near the ILM, breaking its local symmetry, the phase mode and the even-LLM pick up similar symmetry components from the resulting lateral oscillation and a phase oscillation of the ILM. The lower traces in Fig. 5 clearly show the mixing of these two modes. The ILM starts vibrating laterally at larger amplitude. Finally, its range exceeds the lattice constant, it is no longer locked to the driver and disappears.

5. Summary

The local laser modulation method breaks the symmetry of the even-LLMs associated with a driven AR-ILM, so that both are observable. As the frequency of the ILM is shifted toward the lower bifurcation point the even-LLM approaches the odd phase mode of the AR-ILM. The bifurcation point occurs when these two localized modes coalesce. The new transition frequency is shifted, from that of the pure lattice case, due to the presence of the symmetry breaking impurity mode.

References

[1] A. J. Sievers and S. Takeno, "Intrinsic Localized Modes in Anharmonic Crystals", Phys. Rev. Lett. **61**, 970 (1988)

[2] A. J. Sievers and J. B. Page, “Unusual anharmonic local mode systems” in “Dynamical Properties of Solids: Vol. 7, "Phonon Physics, The Cutting Edge", G. K. Norton and A. A. Maradudin, eds., (North Holland, Amsterdam, 1995), p 137.

[3] D. K. Campbell, S. Flach, and Y. S. Kivshar, "Localizing Energy Through Nonlinearity and Discreteness", Physics Today **57**, 43 (2004).

[4] S. Flach and A. Gorbach, "Discrete breathers — Advances in theory and applications", Phys. Repts. **467**, 1 (2008).

[5] T. Rössler and J. B. Page, "Intrinsic localized modes in driven anharmonic lattices with realistic potentials", Phys. Lett. A, **204**, 418 (1995)
[6] M. Sato, B. E. Hubbard, A. J. Sievers, B. Ilic, D. A. Czaplewski and H. G. Craighead, "Observation of locked intrinsic localized vibrational modes in a micromechanical oscillator array", Phys. Rev. Lett. **90**, 044102 (2003)
[7] M. Sato, B. E. Hubbard, and A. J. Sievers, "Nonlinear energy localization and its manipulation in micromechanical oscillator arrays", Rev. Mod. Phys., vol. **78**, 137 (2006).
[8]V. Hizhnyakov, A. Shelkan, M. Klopov, S. A. Kiselev and A. J. Sievers, "Linear local modes induced by intrinsic localized modes in a monatomic chain", Phys. Rev. **B 73**, 224302 (2006).
[9]A. J. Dick, A. J. Balachandran, and C. D. Mote, "Intrinsic localized modes in microresonator arrays and their relationship to nonlinear vibration modes", Nonlin. Dyn. **54**, 13 (2008).
[10] Q. Chen, L. Huang, Y.-C. Lai, and D. Dietz, "Dynamical mechanism of intrinsic localized modes in micromechanical oscillator arrays", Chaos **19**, 013127 (2009).
[11] E. Kenig, B. A. Malomed, M. C. Cross, and R. Lifshitz, "Intrinsic localized modes in parametrically driven arrays of nonlinear resonators", Phys. Rev. **E 80**, 046202 (2009).
[12] J. Wiersig, S. Flach, and K. H. Ahn, "Discrete breathers in ac-driven nanoelectromechanical shuttle arrays", Appl. Phys. Lett. **93**, 222110 (2009).
[13]M. Kimura and T. Hikihara, "Capture and Release of Traveling Intrinsic Localized Mode in Coupled Cantilever Array", Chaos **19**, 013138 (2009).
[14] Y. Doi and K. Yoshimura, "Translational Asymmetry Controlled Lattice and Numerical Method for Moving Discrete Breather in Four Particle System", J. Phys. Soc. Jpn., **78**, 034401 (2009).
[15] L. Q. English, F. Palmero, A. J. Sievers, “Traveling and stationary intrinsic localized modes and their spatial control in electrical lattices," Physical Review **E 81**, 046605 (2010).
[16] M. Sato, S. Imai, N. Fujita, S. Nishimura, Y. Takao, Y. Sada, B. E. Hubbard, B. Ilic, and A. J. Sievers, "Experimental Observation of the Bifurcation Dynamics of an Intrinsic Localized Mode in a Driven 1D Nonlinear Lattice", Phys. Rev. Lett. **107**, 234101 (2011)
[17] Y. Doi and A. Nakatani, "Numerical study on unstable perturbation of intrinsic localized modes in graphene", Journal of Solid Mechanics and Materials Engineering, Vol.**6** No.1, pp.71-80 (2012).
[18] Y. Watanabe, K. Hamada, and N. Sugimoto , "Mobile Intrinsic Localized Modes of a Spatially Periodic and Articulated Structure", J. Phys. Soc. Jpn. **81** (2012) 014002
[19]J. Fajans, E. Gilson, and L. Friedland, "Autoresonant (nonstationary) excitation of a collective nonlinear mode ", Phys. Plasmas **6**, 4497 (1999).
[20]J. Fajans and L. Friedland, "Autoresonant (nonstationary) excitation of pendulums, plutinos, plasmas and other nonlinear oscillators", Am. J. Phys. **69**, 1096 (2001).
[21]S. V. Batalov and A. G. Shagalov, " Control of solitons", Phys. Rev. **E 84**, 016603 (2011).
[22]Y. Gopher, L. Friedland, and A. G. Shagalov, "Multiphase autoresonant excitations in discrete nonlinear Schrödinger systems", Phys. Rev. **E 72**, 036604 (2005).